The Cryosphere Discuss., doi:10.5194/tc-2016-289, 2017
Manuscript under review for journal The Cryosphere
Published: 1 February 2017

Change in Frozen Soils and its Effect on Regional Hydrology in the Upper Heihe Basin, the Northeast Qinghai-Tibetan Plateau

Bing Gao[1], Dawen Yang[2]*, Yue Qin[2], Yuhan Wang[2], Hongyi Li[3], Yanlin Zhang[3], and Tingjun Zhang[4]

[1] School of Water Resources and Environment, China University of Geosciences, Beijing 100083, China

[2] State Key Laboratory of Hydroscience and Engineering, Department of Hydraulic Engineering, Tsinghua University, Beijing 100084, China

[3] Cold and Arid Regions Environmental and Engineering Research Institute, Chinese Academy of Sciences, Lanzhou, Gansu 730000, China

[4] Key Laboratory of West China's Environmental Systems (MOE), College of Earth and Environmental Sciences, Lanzhou University, Lanzhou, 730000, China

* *Correspondence to*: Dawen Yang (yangdw@tsinghua.edu.cn)

The Cryosphere Discuss., doi:10.5194/tc-2016-289, 2017
Manuscript under review for journal The Cryosphere
Published: 1 February 2017

ABSTRACT:

Frozen ground has an important role in regional hydrological cycle and ecosystem, especially on the Qinghai-Tibetan Plateau, which is characterized by high elevation and a dry climate. This study modified a distributed physically-based hydrological model and applied it to simulate the long-term (from 1961 to 2013) change of frozen ground and its effect on hydrology in the upper Heihe basin located at Northeast Qinghai-Tibetan Plateau. The model was validated carefully against data obtained from multiple ground-based observations. The model results showed that the permafrost area shrank by 9.5% (approximately 600 km^2), especially in areas with elevation between 3500 m and 3900 m. The maximum frozen depth of seasonally frozen ground decreased at a rate of approximately 4.1cm/10yr, and the active layer depth over the permafrost increased by about 2.2 cm/10yr. Runoff increased significantly during cold seasons (November-March) due to the increase in liquid soil moisture caused by rising soil temperature. Areas where permafrost changed into the seasonally frozen ground at high elevation showed especially large changes in runoff. Annual runoff increased due to increased precipitation, the base flow increased due to permafrost degradation, and the actual evapotranspiration increased significantly due to increased precipitation and soil warming. The groundwater storage showed an increasing trend, which indicated that the groundwater recharge was enhanced due to the degradation of permafrost in the study area.

KEYWORDS: permafrost; frozen ground; active layer, soil moisture; soil temperature; runoff, distributed hydrological model

1. Introduction

Hydrological processes on the Qinghai-Tibetan Plateau, which is characterized by high elevation and cold climate are greatly influenced by cryosphere processes. In recent years, the runoff change in the Qinghai-Tibetan Plateau has received increasing attentions due to its significant effect on water resources and the ecosystem (Cuo et al., 2014). The change in frozen soils and its effect on hydrological processes is a key scientific issue (Yang et al., 2010; Cheng and Jin, 2013). Frozen soils including permafrost and seasonally frozen ground, have active interactions with land surface hydrological processes. Changes in frozen soils alter land surface infiltration, soil drainage, and subsurface water storage and influences the partition of direct surface runoff and subsurface flow. Hydrological changes caused by frozen soils can greatly impact land-atmosphere interactions and thus the water balance and energy balance of the land surface. Understanding the changing frozen soil conditions and their impact on hydrological processes is important for water resources management and ecosystem protection on the Qinghai-Tibetan Plateau.

Several previous observation-based studies have examined long-term changes in frozen soils and their impacts on hydrological processes. Some studies reported that permafrost thawing might enhance base flow, especially runoff in winter in the Arctic and the Subarctic (Walvoord et al., 2016; Jacques and Sauchyn, 2009; Ye et al., 2009) and in Northeast China (Liu et al., 2003). A few studies argued that permafrost thawing might reduce river runoff (Qiu, 2012). These studies used either in-situ observations in experimental catchments or long-term meteorological observations. Field experiments are usually at the plot scale for a short period, which might lose the spatial variability and long-term trends, and the long-term meteorological observations do not provide data on soil freezing and thawing processes (McClelland et al., 2004; Liu et al., 2003; Niu et al., 2011). Previous observation-based studies focus either on runoff trends or changes in frozen soils; few studies thoroughly discuss the relationship between runoff trends and changes in frozen soils. The impact of the change in frozen soils on regional hydrological processes is not fully understood based on the existing observations and it is difficult to attribute the long-term trends of streamflow to the change in frozen soils (Woo et al., 2008).

Hydrological models have been widely used to analyze the regional hydrological changes under changing environmental conditions; however most hydrological models do not consider the freezing-thawing processes in soil. Some studies incorporate simple freezing-thawing schemes into the hydrological models (Rawlins et al., 2003; Chen et al., 2008), but do not simulate the soil thermal fluxes. The SiB2 model (Sellers et al., 1996), the modified VIC model (Cherkauer and Lettenmaier, 1999) and the CLM model (Oleson et al., 2010) consider the land surface energy balance and soil heat transfer processes, but do not represent the complex landscape at the catchment scale. The GEOtop model simulates the three-dimensional water flux and vertical heat transfer in soil, but it is difficult to apply at the regional scale. Wang et al. (2010) and Zhang et al. (2013) incorporated frozen soil schemes in a distributed hydrological model and showed improved performance in a small mountainous catchment. Rawlins et al. (2013) analyzed the impact of future climate change at 4 sites in Alaska. Subin et al. (2013)

and Lawrence et al. (2015) used the CLM model to simulate the change in permafrost at global scale. Cuo et al. (2015) simulated frozen soil degradation and its effects on surface hydrology at the plot scale using the VIC model. The previous modelling studies focused on simulations of the changes in frozen soils and the hydrological impacts at either the small scale or global/continental scale. Regional modelling studies linking the frozen soils changes and hydrological responses were inadequate.

The Qinghai-Tibetan Plateau is the Asian water tower, and water availability on the plateau is very important for water supply and food security in the downstream regions with large populations (Walter et al., 2010). Different from the Arctic and Subarctic, the permafrost thickness on the Qinghai-Tibetan Plateau is relatively thin and warm, and the frozen depth of the seasonally frozen soils is also shallow (Yang et al., 2010). Therefore, frozen soil processes in the Qinghai-Tibetan Plateau are more sensitive to rising air temperature (Yang et al., 2010). Due to the drier climate and warmer soil, the frozen soil processes are more closely related to the hydrological processes on the Qinghai-Tibetan Plateau than they are in the Arctic and Subarctic regions. There is also higher spatial variability in topography and landscapes on the Qinghai-Tibetan Plateau where the permafrost and seasonally frozen ground coexist.

An evident increase in the annual and seasonal air temperature has been observed in the Qinghai-Tibetan Plateau (Li et al., 2005; Liu and Chen, 2000; Zhao et al., 2004). Several studies have shown changes in frozen soils based on the long-term observations. For example, Cheng and Wu (2007) analyzed the borehole observations of soil temperature profiles on the Qinghai-Tibetan Plateau and found that the active layer thickness of frozen soils increased by 0.15-0.50 m during the period of 1996-2001. Zhao et al. (2004) found a decreasing trend of freezing depth in the seasonal frozen soils using observations from 50 stations. Several studies analyzed the relationship between the change in frozen soils and streamflow based on observed data (Zhang et al., 2003; Jin et al., 2009; Niu et al., 2011). However, these studies have not addressed the spatial and temporal variations of the frozen soils. The spatio-temporal characteristics of the long-term change in frozen soils is not sufficiently clear. The magnitude of the effect of frozen soils on regional hydrology remains unclear, and the modelling studies on frozen soils changes and their hydrological impacts are insufficient. Therefore, integrated study based on the long term simulation of soil freezing/thawing processes and the hydrological responses is needed.

Through a comprehensive experiment (Li et al., 2013) in a major research plan entitled “Integrated research on the ecohydrological processes of the Heihe basin” funded by the National Natural Science Foundation of China (NSFC) (Cheng et al., 2014), this study aims: (1) to develop a distributed hydrological model coupling the cryosphere processes especially the soil freezing-thawing processes; (2) to simulate the spatial and temporal changes in frozen soils and to analyze the effects of frozen soils change on hydrological processes in the upper Heihe basin located on the Northeastern Qinghai-Tibetan Plateau.

2. Study area and data

2.1 The Heihe River and upper Heihe basin

The Heihe River is one of the major inland basins in Northwest China. As shown in

The Cryosphere Discuss., doi:10.5194/tc-2016-289, 2017
Manuscript under review for journal The Cryosphere
Published: 1 February 2017

Figure 1, the upper reaches of Heihe River are located on the Northeastern Qinghai-Tibetan Plateau at an elevation of 2200-5000 m and with a drainage area of 10009 km^2, it supplies most of the water resources to the middle and lower reach (Cheng et al., 2014). The annual precipitation in the upper Heihe basin ranges from 200 to 700 mm, and the annual mean air temperature ranges from -9 to 5℃. Permafrost dominates high elevation region above 3700 m (Wang et al., 2013) and seasonal frozen ground covers other parts of the study area. Glaciers are found at an elevation above 4000 m, covering approximately 0.8% of the upper Heihe basin. There are two tributaries (East and West Tributaries) in the upper Heihe basin, on which two hydrological stations are located, namely, Qilian (on the east tributary) and Zhamashike (on the west tributary). The outlet of the upper Heihe basin has a hydrological station, namely Yingluoxia (see Figure 1).

2.2 Data used in the study

(1) Input data of the model

The atmosphere forcing data used to drive the hydrological model include a 1-km resolution gridded dataset of daily precipitation, air temperature, sunshine hours, wind speed and relative humidity. The gridded daily precipitation is interpolated from observations at meteorological stations (see Figure 1) provided by the China Meteorological Administration (CMA) using the method developed by Shen and Xiong (2015). The other atmosphere forcing data are interpolated by observations at meteorological stations using the inverse distance weighted method. The interpolation of air temperature considers the temperature gradient with elevation which is provided by the HiWATER experiment (Li et al., 2013).

The Cryosphere Discuss., doi:10.5194/tc-2016-289, 2017
Manuscript under review for journal The Cryosphere
Published: 1 February 2017

The land surface data used to build the model include land use, topography, leaf area index, and soil parameters. The topography data are obtained from the SRTM dataset (Jarvis et al., 2008) with a spatial resolution of 90 m. The land use/cover data are provided by the Institute of Botany, Chinese Academy of Sciences (Zhou and Zheng, 2014). The leaf area index (LAI) data with 1-km resolution are obtained from the dataset developed by Fan (2014). The soil water parameters and soil physical parameters of each grid are obtained from the 1-km dataset developed by Song et al. (2016), which includes the saturated hydraulic conductivity, residual soil moisture content, saturated soil moisture content, soil sand matter content, soil clay matter content and soil organic matter content.

(2) Data used for model calibration and validation

This study uses the observed daily river discharge data at the Yingluoxia, Qilian and Zhamashike stations, the daily soil temperature of different depths at the Qilian station and the daily frozen depths at the Qilian and Yeniugou stations for model calibration and validation. Daily river discharge data are obtained from the Hydrology and Water Resources Bureau of Gansu Province. Daily soil temperature data observed at the Qilian station which is from January 1, 2004 to December 31, 2013 and daily frozen depth data observed at the Qilian and Yeniugou station from January 1, 2002 to December 31, 2013 are provided by CMA.

To investigate the spatial distribution of permafrost, boreholes were drilled during the NSFC major research plan. Temperature observations at six boreholes, whose location are shown in Figure 1, are provided by Wang et al. (2013). The borehole depth is 100 m for T1, 69 m for T2, 50 m for T3 and 90 m for T4, and 20 m for T5 and T7. Monthly actual evapotranspiration data with 1-km resolution during the period of 2002-2012 estimated using remote sensing data (Wu et al., 2012; Wu, 2013) are used to evaluate the model-simulated evapotranspiration. We also used field observations of the hourly liquid soil moisture to validate the model simulation of frozen soils. The HiWATER experiment (Li et al., 2013; Liu et al., 2011) provided the soil moisture data observed at the A'rou Sunny Slope station (100.52 E, 38.09 N), which is available from January 1, 2014 to December 31, 2014.

3. Methodology

3.1 Brief introduction of the hydrological model

This study used a distributed hydrological model GBEHM (geomorphology-based ecohydrological model), which was developed in an integrated research project under the major research plan of "Integrated research on the ecohydrological process of the Heihe River Basin" (Yang et al., 2015; Gao et al., 2016). The GBEHM used 1-km grid system to discretize the study catchment. Based on the 1-km digital elevation model (DEM), the study catchment was divided into 251 sub-catchments. A sub-catchment was further divided into flow-intervals along the main stream of the sub-catchment (Yang et al., 2015). To capture the sub-grid topography, the grid was represented by a number of hillslopes with an average length and gradient, but different aspect, which were estimated from the 90-m DEM. The terrain properties of a hillslope include the slope length and gradient, slope aspect, the soil type and vegetation type (Yang et al., 2015).

The Cryosphere Discuss., doi:10.5194/tc-2016-289, 2017
Manuscript under review for journal The Cryosphere
Published: 1 February 2017

The Cryosphere Discussions

The hillslope is the basic unit for the hydrological simulation, on which the water and heat transfer (both of conduction and convection) in the vegetation canopy, snow cover/glacier, soil layers are simulated. The canopy interception, radiation transfer in the canopy and the energy balance of the land surface are described using the methods developed in SIB2 (Sellers et al., 1985, 1996). The surface runoff on the hillslope is solved using the kinematic wave equation. The groundwater aquifer is considered an individual storage corresponding to each grid. Exchange between the groundwater and the river water is calculated using Darcy's law (Yang et al., 1998, 2002).

The model runs with a time step of 1 hour. Runoff generated from the grid is the lateral inflow into the river at the same flow interval in the corresponding sub-catchment. Flow routing in the river network is calculated using the kinematic wave equation following the sequence determined by the Horton-Strahler scheme (Yang et al., 1998, 2015).

3.2 Simulation of cryospherical processes

The simulation of cryosphere processes in GBEHM includes glacier ablation, snow melt, and soil freezing and thawing.

(1) Glacier ablation

Glacier ablation is simulated using an energy balance model (Oerlemans, 2001) as:

$$Q_M = SW(1-\alpha) + LW_{in} - LW_{out} - Q_H - Q_L - Q_G + Q_R \quad (1)$$

where Q_M is the net energy absorbed by the surface of the glacier (W/m^2); SW is the incoming shortwave radiation (W/m^2); α is the surface albedo; LW_{in} is the incoming longwave radiation (W/m^2); LW_{out} is the outgoing longwave radiation (W/m^2); Q_H is the sensible heat flux (W/m^2); Q_L is the latent heat flux (W/m^2); Q_R is the energy from rainfall (W/m^2); and Q_G is the penetrating shortwave radiation (W/m^2). The surface albedo is calculated as (Oerlemans and Knap, 1998):

$$\alpha = \alpha_{snow} + (\alpha_{ice} - \alpha_{snow}) e^{-h/d^*} \tag{2}$$

where α_{snow} is the albedo of snow on the glacier surface; α_{ice} is the albedo of the ice surface; h is the snow depth on the glacier surface (m); $d*$ is a parameter of the snow depth effect on the albedo (m).

The amount of melt water is calculated as (Oerlemans, 2001):

$$M = \frac{Q_M}{L_f} dt \tag{3}$$

where dt is the time step used in the model (s) and L_f is the latent heat of fusion (J/kg).

(2) Snow melt

A multi-layer snow cover model is used to describe the mass and energy balance of snow cover. For each snow layer, temperature is solved using an energy balance approach (Bartelt and Lehnin, 2002):

$$C_s \frac{\partial T_s}{\partial t} - L_f \frac{\partial \rho_i \theta_i}{\partial t} = \frac{\partial}{\partial z}(K_s \frac{\partial T}{\partial z}) + \frac{\partial I_R}{\partial z} + Q_R \tag{4}$$

where C_s is the heat capacity of snow (J m^{-3} K^{-1}); T_s is the temperature of the snow layer (K); ρ_i is the density of the ice (kg/m^3); θ_i is the volumetric ice content; K_s is the thermal conductivity of snow (W m^{-1} K^{-1}); L_f is the latent heat of ice fusion (J/kg) ; I_R is the radiation transferred into the snow layer (W/m^2) and Q_R is the energy brought by rainfall (W/m^2) which is only considered for the top snow layer. The solar radiation transfer in the snow layers and the snow albedo are simulated using the SNICAR model which is solved using the method developed by Toon et al. (1989). Eq.

The Cryosphere Discuss., doi:10.5194/tc-2016-289, 2017
Manuscript under review for journal The Cryosphere
Published: 1 February 2017

(4) is solved using a finite differential scheme.

The mass balance of the snow layer is described as (Bartelt and Lehnin, 2002):

$$\frac{\partial \rho_i \theta_i}{\partial t} + M_{iv} + M_{il} = 0 \quad (5)$$

$$\frac{\partial \rho_l \theta_l}{\partial t} + \frac{\partial U_l}{\partial z} + M_{lv} - M_{il} = 0 \quad (6)$$

where ρ_l is the density of the liquid water (kg/m^3); θ_l is the volumetric liquid water content; U_l is the liquid water flux (kg m^{-2} s^{-1}); M_{iv} is the mass of ice that is changed into vapor within a time step (kg m^{-3} s^{-1}); M_{il} is the mass of ice that is changed into liquid water within a time step (kg m^{-3} s^{-1}); and M_{lv} is the mass of liquid water that is changed into vapor within a time step (kg m^{-3} s^{-1}). The liquid water flux of the snow layer is calculated as (Jordan, 1991):

$$U_l = -\frac{K_l}{\mu_l} \rho_l^2 g \quad (7)$$

where K_l is the hydraulic permeability (m^2), μ_l is dynamic viscosity of water at 0 ℃ (1.787×10^{-3} N s/m^2), ρ_l is the density of liquid water (kg/m^3) and g is gravitational acceleration (m/s^2). The water flux of the bottom snow layer is considered snowmelt runoff.

(3) Soil freezing and thawing

The energy balance of the soil layer is solved as (Flerchinger and Saxton, 1989):

$$C_s \frac{\partial T}{\partial t} - \rho_i L_f \frac{\partial \theta_i}{\partial t} - \frac{\partial}{\partial z}\left(\lambda_s \frac{\partial T}{\partial z}\right) + \rho_l c_l \frac{\partial q_l T}{\partial z} = 0 \quad (8)$$

where C_s is the volumetric soil heat capacity (J m^{-3} K^{-1}); T is the temperature (K) of the soil layers, z is the vertical depth of the soil (m); θ_i is the volume ice content; ρ_i is the density the ice (kg/m^3); λ_s is the thermal conductivity (W m^{-1} K^{-1}); ρ_l is the density of liquid water (kg/m^3); and c_l is the heat capacity of liquid water (J kg^{-1} K^{-1}).

The Cryosphere Discuss., doi:10.5194/tc-2016-289, 2017
Manuscript under review for journal The Cryosphere
Published: 1 February 2017

In addition, q_l is the water flux between different soil layers (m/s) and is solved using the 1-D Richards equation. The unsaturated soil hydraulic conductivity is calculated using the modified van Genuchten's equation (Wang et al., 2010) as:

$$K = f_{ice} K_{sat} (\frac{\theta_l - \theta_r}{\theta_s - \theta_r})^{1/2} [1-(1-(\frac{\theta_l - \theta_r}{\theta_s - \theta_r})^{-1/m})^m]^2 \quad (9)$$

where K is the unsaturated soil hydraulic conductivity (m/s); K_{sat} is the saturated soil hydraulic conductivity; θ_l is the volumetric liquid water content; θ_s is the saturated water content; θ_r is the residual water content; m is an empirical parameter in van Genuchten's equation and f_{ice} is an empirical hydraulic conductivity reduction factor which is calculated using soil temperature as (Wang et al., 2010):

$$f_{ice} = \exp[-10(T_f - T_{soil})], \quad 0.05 \le fice \le 1 \quad (10)$$

where T_f is 273.15 K and T_{soil} is the soil temperature.

Eq. (8) solves the soil temperature with the upper boundary condition as the heat flux into the top surface soil layer. When the ground is not covered by snow, the heat flux from the atmosphere into the top soil layer is expressed as (Oleson et al., 2010):

$$h = S_g + L_g - H_g - \lambda E_g + Q_R \quad (11)$$

where h is the upper boundary heat flux into the soil layer (W m^{-2}); S_g is the solar radiation absorbed by the top soil layer (W m^{-2}); L_g is the net long wave radiation absorbed by the ground (W m^{-2}), H_g is the sensible heat flux from the ground (W m^{-2}); λE_g is the latent heat flux from the ground (W m^{-2}); and Q_R is the energy brought by rainfall (W/m^2). When the ground is covered by snow, the heat flux into the top soil layer is calculated as:

$$h = I_p + G \quad (12)$$

where I_p is the radiation that penetrates the snow cover, and G is the heat conduction from the bottom snow layer to the top soil layer. Eq (8) is solved using a finite differential scheme with an hourly time step.

To simulate the permafrost we consider an underground depth of 50 m and assume the bottom boundary condition as zero heat flux exchange. The vertical soil column is divided into 39 layers in the model. The topsoil of 1.7 m is subdivided into 9 layers. The first layer is 5 cm and the soil layer thickness increases linearly from 5 cm to 30 cm up to the depths of 0.8 m and then decreases linearly to 10 cm up to the depths of 1.7 m. There are 12 soil layers from 1.7 m to 3.0 m with a constant thickness of 10 cm. From the depth of 3 m to 50 m, there are 18 layers with thickness increasing exponentially from 10 cm to 12 m. The liquid soil moisture, ice content, and soil temperature of each layers are calculated at each time step. The soil heat capacity and soil thermal conductivity are estimated using the method developed by Farouki (1981).

3.3 Model calibration

In this study, model simulation during the period of 1961-2001 was used to spin up to specify the initial values of the hydrological variables (e.g., soil moisture, soil temperature, soil ice content, groundwater table, etc.). The period of 2002-2006 was used for model calibration and the period of 2008-2012 was for model validation. The daily soil temperature at the Qilian station and the frozen depths at the Qilian and Yeniugou stations were used to calibrate the soil reflectance according to vegetation type. The other parameters such as groundwater conductivity were calibrated according to the streamflow discharge in the winter season. We calibrated the surface retention

The Cryosphere Discuss., doi:10.5194/tc-2016-289, 2017
Manuscript under review for journal The Cryosphere
Published: 1 February 2017

capacity and surface roughness to match the observed flood peaks, and calibrated the leaf reflectance, leaf transmittance and maximum Rubsico capacity of the top leaf based on the remote sensing evapotranspiration data. Table 1 shows the major parameters used in the model.

4. Results

4.1 Validation result

Figure 2 shows the comparison of the model-simulated and observed soil temperature profiles at six boreholes. The model successfully captured the vertical distribution of the soil temperature at T1, T2, T3 and T4 in the permafrost area, but there were some overestimations above 20 m. The errors in simulating the vertical temperature profile near the surface might be due to simplification of the 3-D topography. At T5 located in seasonally frozen ground, the simulated soil temperature profile from approximately 4 m to 20 m does not agree well with the observed one. This error might be related to the heterogeneity of soil properties especially the thermal conductivity and heat capacity, which might not be accurately described by the current data. The model simulation agrees well with the borehole observation at T7, which is located at the transition zone from permafrost to seasonally frozen ground. This implies that the model well identified the lower limit of permafrost.

We also validated model simulation of the freezing/thawing cycles based on long-term observations of soil temperature and frozen depth. Figure 3 compares the simulated soil temperature with the observed temperature at the Qilian station, which is located in the seasonally frozen ground (observed daily soil temperature data are available since 2004). Generally, the model simulations accurately captured the changes in soil temperature profile. Validation of the soil temperature at different depths (5 cm, 10 cm, 20 cm, 40 cm, 80 cm, 160 cm, and 320 cm) showed that the root mean square errors decreases with increasing depth. The errors was approximately 3℃ for the top three depths (5 cm, 10 cm and 20 cm). The error for depths of 40 cm and 80 cm was 2.5℃ and 1.9℃, respectively, and the error was 0.9℃ at a depth of 3.2 m. We compared the model-simulated daily frozen depth with in-situ observations at the Qilian and Yeniugou Stations from 2002 to 2014, as shown in Figure 4. The model accurately reproduced the daily variations in frozen depth although the depth was underestimated by approximately 50 cm at the Yeniugou station. In general, the validation of soil temperature and frozen depth indicates that the model well captured the freezing and thawing processes in the upper Heihe basin.

The observed hourly liquid soil moisture at the A’rou Sunny Slope station was used as an independent additional validation. Figure 5 shows the comparison between the simulated and observed liquid soil moisture at different depths from January 1 to December 31 in 2014. The model simulation agreed well with the observed liquid soil moisture during the freezing and thawing processes at different depths. However, relatively larger errors existed in the simulations at a depth of 4 cm, which might be related to the heterogeneity along the soil column that was not fully addressed in the model.

Figure 6 compares the model simulated and the observed daily streamflow discharge at the Yingluoxia, Qilian and Zhamashike station. The model simulation agreed well with the observations. The model simulation captured the flood peaks and the magnitude of base flow in both of the calibration and validation periods. In the calibration period, the Nash-Sutcliffe efficiency (NSE) coefficient was 0.64, 0.65 and 0.70 for the Yingluoxia, Qilian and Zhamashike stations, respectively. In the validation period, the NSE value were 0.65, 0.60, and 0.75. The relative error (RE) was within 10% for both the calibration and validation period (see Table 2). Figure 7 shows the comparison of the model-simulated monthly actual evaporation and remote sensing-based evaporation data for the entire calibration and validation periods. The GBEHM simulation showed similar temporal variations in actual evapotranspiration compared with the remote sensing based estimation, and the root mean square error (RMSE) of the simulated monthly evapotranspiration was 8.0 mm in the calibration period and 6.3 mm in the validation period. These validation results indicate that the model accurately simulates the cryosphere hydrological processes in the upper Heihe basin.

4.2 Long-term changes in freezing-thawing processes and frozen soils

The freezing-thawing and hydrological processes of the upper Heihe basin from 1961 to 2013 were simulated by GBEHM. A 50-year run which repeated the atmosphere forcing in the period of 1961-1970 was used to obtain the initial conditions. The long-term changes in frozen soils, runoff and soil moisture were analyzed based on the model simulation.

In the upper Heihe basin, the ground surface starts freezing in November and thawing in April (Wang et al., 2015a). From November to March, the ground surface temperature is below 0℃ in both the permafrost and seasonally frozen ground regions,

The Cryosphere Discuss., doi:10.5194/tc-2016-289, 2017
Manuscript under review for journal The Cryosphere
Published: 1 February 2017

and precipitation mainly falls in the period from April to October. Therefore, a year is subdivided into two seasons, i.e., the freezing season (November to March) and the thawing season (April to October) to investigate the changes in frozen soils and their hydrological impact. Increasing of precipitation and air temperature in the study area in both seasons in the past 50 years was reported in a previous study (Wang et al., 2015b).

Figure 8 shows the changes in the basin-averaged soil temperature in the freezing and thawing seasons. The soil temperature increased in all seasons especially in the past 30 years. The increasing trend of soil temperature was larger in the freezing season than in the thawing seasons. In the freezing season (Figure 8(a)), the top layer soil temperature was lower than the deep layer soil temperature. The linear trend of the top layer (0-0.5 m) soil temperature was 0.31℃/10yr and the trend of the deep layer (2.5-3 m) soil temperature was 0.22℃/10yr. The soil temperature in deep layer (2.5-3 m) changed from -1.1℃ in the 1960s to near 0℃ in the most recent decade. In the thawing season (see Figure 8(b)), the increasing trend of the top layer (0-0.5 m) soil temperature (0.17℃/10yr) was greater than the trend of the deep layer (2.5-3 m) soil temperature (0.10℃/10yr).

Permafrost is defined as ground with a temperature at or below 0℃ for at least two consecutive years (Woo, 2012). This study differentiated permafrost from seasonally frozen areas based on the simulated vertical soil temperature profile. For each year, the frozen soil condition was determined by searching the soil temperature profile within a four-year window from the previous three years to the current year. Figure 9 shows the area change of the permafrost during 1961-2013. As shown in Figure 9 (a), the

The Cryosphere Discuss., doi:10.5194/tc-2016-289, 2017
Manuscript under review for journal The Cryosphere
Published: 1 February 2017

permafrost areas decreased approximately 9.5% (6445 km^2 in the 1970s and 5831 km^2 in the 2000s), indicating evident degradation of the permafrost in the upper Heihe basin in the past 50 years.

Figure 9 (b) shows the changes in the basin-averaged maximum frozen depth for the seasonally frozen ground and active layer thickness over the permafrost. The basin-averaged annual maximum frozen depth showed a significant decreasing trend (4.1 cm/10yr). In addition, the maximum frozen depth had a significantly negative correlation with the annual mean air temperature (r = -0.73). In contrast, an increasing trend of active layer thickness in the permafrost regions was observed (2.2 cm/10yr), which had a significantly positive correlation with the annual mean air temperature.

Figure 10 shows the frozen soils distributions in the period of 1971-1980 and in the period of 2001-2010. Comparing the frozen soils distributions in the two periods, major changes in frozen soils were observed on the sunny slopes at elevation between 3500 and 3700 m, especially in the west tributary, where large areas of permafrost changed into seasonally frozen ground.

Figure 11 shows the monthly mean soil temperature over the areas with elevation between 3300 and 3500 m and over areas with elevation between 3500 and 3700 m in the upper Heihe basin. In the areas with elevation between 3300 and 3500 m located in the seasonally frozen ground region, as shown in Figure 11(a), the frozen depth decreased and the soil temperature in the deep layer (with depth greater than 2 m) increased. Figure 11(b) shows that the increase in soil temperature was larger in the area with higher elevation (3500-3700 m). This figure shows that the thickness of the permafrost layer decreased as soil temperature increased, and the permafrost changed into seasonally frozen ground after 2000.

4.3 Changes in the water balance and the hydrological processes

Table 3 shows the decadal changes in the annual water balance from 1961 to 2010 based on the model simulation. The annual precipitation, annual runoff and annual runoff ratio had the same decadal variation; however the annual evapotranspiration maintained an increasing trend since the 1970s which was consistent with the rising air temperature and soil warming. Although the actual evapotranspiration increased, the runoff ratio remained stable during the 5 decades because of the increased precipitation.

The changes in runoff (both simulated and observed) in different seasons are shown in Figure 12 and Table 4. The model-simulated and observed runoff both showed a significant increasing trend in the freezing season and in the thawing season. This indicates that the model simulation accurately reproduced the observed long-term changes. In the freezing season, since there was no glacier melt and snow melt (see Table 4), runoff was mainly the subsurface flow. In the thawing season, as shown in Table 4, snowmelt runoff contributed approximately 16% of the total runoff and glacier runoff contributed only a small fraction of total runoff (approximately 2.4%). Therefore, rainfall runoff was the major component of total runoff in the thawing season, and the runoff increasing in the thawing season was mainly due to increased rainfall runoff. As shown in Figure 12, the actual evapotranspiration increased significantly in both seasons due to increased precipitation and soil warming. The increasing trend of the actual evapotranspiration was higher in the thawing season than in the freezing season,

The Cryosphere Discuss., doi:10.5194/tc-2016-289, 2017
Manuscript under review for journal The Cryosphere
Published: 1 February 2017

which indicates that the actual evapotranspiration was limited by the water available in this region.

Figure 13 shows the changes in the basin-averaged annual water storage in the top 0-3 m layer and the groundwater storage. The annual liquid water storage of the top 0-3 m showed a significant increasing trend especially in the most recent 3 decades. This long-term change in liquid water storage was similar to the runoff change in the freezing season, as shown in Figure 12 (a), with a correlation coefficient of 0.80. The annual ice water storage in the top 0-3 m soil showed significant decreasing trend due to frozen soils changes. Annual groundwater storage showed a significantly increasing trend especially in the most recent 3 decades, which indicates the groundwater recharge increases with the frozen soil degradation.

5. Discussion

5.1 Impact of frozen soils changes on the soil moisture and runoff

Figure 14 shows the spatial-averaged liquid soil moisture changes in the region covered by seasonally frozen ground with elevation between 3300 and 3500 m and in the area with elevation between 3500 and 3700 m where the permafrost changed into seasonally frozen ground. In the seasonally frozen ground with elevation of 3300-3500 m (Figure 14(a)), by comparing with the soil temperature shown in Figure 11 (a), we can see that the liquid soil moisture increase was mainly caused by the decrease in the frozen depth. The liquid soil moisture in the deep soil layer increased significantly since 1990s (see Figure 14(b)) in the area with elevation of 3500-3700 m where the permafrost changed to seasonally frozen ground. Compared with the soil temperature change shown in Figure 11 (b), the liquid soil moisture increases in this region was mainly caused by the change of permafrost to seasonally frozen ground, indicating that the frozen soils degradation caused a significant increase in liquid soil moisture. Therefore, the basin-averaged liquid soil moisture was highly correlated with the soil temperature in the freezing seasons as shown in Table 5. The liquid soil moisture was also highly correlated with soil temperature in the thawing season, because of the increase in the active layer thickness of the permafrost and degradation of the permafrost (i.e., the change from permafrost to seasonally frozen ground). This correlation was larger than the correlation between liquid soil moisture and precipitation because the liquid soil moisture increase caused by the permafrost degradation is more significant than the liquid soil moisture increase caused by increased precipitation in the thawing season.

In the freezing season, since the surface ground is frozen, runoff is mainly subsurface flow coming from seasonally frozen ground. Table 5 shows that runoff has the highest correlation with the liquid soil moisture in the freezing season, which indicates that the frozen soils change was the major cause of the increased liquid soil moisture, resulting in increased runoff in the freezing season. During the past 50 years, parts of the permafrost changed into seasonally frozen ground, and the thickness of the seasonally frozen ground decreased, which led to increased liquid soil moisture in the deep layers during the freezing season as shown in Figure 14. The increase in liquid soil moisture also increased the hydraulic conductivity which enhanced the subsurface flow.

In the thawing season from April to October, the thickness of the seasonally frozen ground rapidly decreased to zero and the thaw depth of permafrost reached the maximum. Runoff in the thawing season was mainly rainfall runoff as shown in Table 4. Table 5 shows that runoff was more strongly correlated with precipitation and relatively more weakly correlated with liquid soil moisture, which illustrates that the increased runoff mainly came from increased precipitation in the thawing season. The correlation between runoff and liquid soil moisture in the thawing season was mainly due to the high correlation between the liquid soil moisture and the precipitation.

Figure 15 shows the changes in areal mean runoff along the elevation for different seasons. There was a large difference in runoff variation with the elevation during the different seasons. In the freezing season, the runoff change from the 1970s to the 2000s in the region of seasonally frozen ground (mainly located below 3500 m, see Figure 10) was relatively small. Runoff in the areas with elevation of 3500-3900 m showed larger change. This is due to the shift from permafrost to seasonally frozen ground in some areas with elevation range of 3500-3900 m as simulated by the model, particularly for the sunny hillslopes (see Figure 10). This illustrates that a change from the permafrost to the seasonally frozen ground has a larger impact on the runoff than a change in frozen depth in seasonally frozen ground. In the thawing season runoff increased with elevation due to the increase in precipitation with increasing elevation, and the runoff increase was mainly determined by increased precipitation (Gao et al., 2016). Precipitation in the region with elevation below 3100 m was low but air temperature was high. Runoff in this region decreased during 2001-2010 compared to 1971-1980 because of higher evapotranspiration.

5.2 Comparison with the previous similar studies

In this study, the model simulation showed that changes in frozen soils led to increased freezing season runoff and base flow in the upper Heihe basin. This result is consistent with previous findings based on the trend analysis of streamflow observations in high latitude regions (Walvoord et al., 2016; Jacques and Sauchyn, 2009; Ye et al., 2009) and in Northeast China (Liu et al., 2003). However, those studies lacked of spatial variability. This study found that the impact of the change in frozen soils on runoff had regional characteristics. In the upper Heihe basin (see Figure 15), a change in frozen soils led to the increased runoff at higher elevations but led to decreased runoff at lower elevation region during the freezing season. This implies that change of the freezing season runoff was controlled by the permafrost degradation in higher elevation region but by the evaporation increase in the lower elevation region due to the air temperature rising. However, runoff at the basin scale mainly came from the higher elevation regions.

This study also showed that the change in frozen soils increased the soil moisture in the upper Heihe basin, which is consistent with the finding of Subin et al. (2013) using the CLM model simulation in north latitude permafrost regions, and the findings of Cuo et al. (2015) using VIC model simulation at 13 sites on the Tibetan Plateau. However, Lawrence et al. (2015) found that permafrost thawing caused soil moisture drying based on CLM model simulations for the global permafrost region. This might be related to the uncertainties in the soil water parameters and the highly spatial heterogeneity of soil properties, which are difficult to consider in a global-scale model. Subin et al. (2013)

and Lawrence et al. (2015) modelled the soil moisture changes in the active layer of permafrost in large areas with coarse spatial resolution. This study revealed the spatio-temporal variability of soil moisture with high spatial resolution and analyzed the correlations with the change in frozen soils.

Wu and Zhang (2010) focused on the changes in the active layer thickness at 10 sites in the permafrost region on the Tibetan Plateau and found a significant increasing trend during the period of 1995-2007, which is consistent with the result of this study. Jin et al. (2009) found decreased soil moisture and runoff due to the permafrost degradation based on observation at the plot scale in the source areas in the Yellow River basin. This result is different from the present study, possibly due to the difference of hydrogeological structure and the soil hydraulic parameters in the source area of Yellow River from those in the upper Heihe basin. Wang et al. (2015a) focused on the change in the seasonally frozen ground in the Heihe River basin based on plot observations, and the increasing trend of the maximum frozen depth was estimated as 4.0 cm/10yr during 1972-2006, which is consistent with the GBEHM model simulation in this study. The increase in groundwater storage illustrated in this study is also consistent with the finding of Cao et al. (2012) based on the GRACE data which showed that groundwater storage increased during the period of 2003~2008 in the upper Heihe basin.

5.3 Uncertainty in the frozen soil simulation

Estimation of the change in permafrost area is a great challenge due to the complex climatology, vegetation, geology. Different methods produce large differences in their estimation results. Jorgenson et al. (2006) found a 4.4% decrease in the area of permafrost in Arctic Alaska from 1982 to 2001 based on airphotos analysis. Wu et al. (2005) reported that the permafrost area decreased by 12% from 1975 to 2002 in the Xidatan basin, Qinghai-Tibetan Plateau based on a ground penetration radar survey. Jin et al. (2006) found an area reduction of 35.6% in island permafrost in Liangdaohe, which is located at the southern Qinghai–Tibet Highway, from 1975 to 1996. Chasmer et al. (2010) found a 30% reduction of the discontinuous permafrost area in the Northwest Territories, Canada from 1947 to 2008 based on remote sensing. This study conducted an integrated simulation of permafrost change and regional hydrological change. Compared with the site observation of Wang et al. (2013) shown in Figure 2, this model slightly overestimated the soil temperature in permafrost areas, which might lead to overestimation of the rate of permafrost area reduction.

There were two major uncertainties in the frozen soils simulation: uncertainty in the land surface energy balance simulation and uncertainty in the simulation of the soil heat-water transfer processes. Uncertainty in the land surface energy balance simulation might result from the estimations of radiation and surface albedo due to the complex topography, vegetation cover and soil moisture distribution, which may induce uncertainties in the estimated ground temperature and thermal heat flux into the deep layers. The uncertainty in simulation of soil heat-water transfer processes might result from the soil water and heat parameters and the bottom boundary condition of heat flux. Permafrost degradation is closely related to the thermal properties of rocks and soils, geothermal flow and initial soil temperature and soil ice conditions. The lack of observed initial condition data could also cause uncertainty in the permafrost change

The Cryosphere Discuss., doi:10.5194/tc-2016-289, 2017
Manuscript under review for journal The Cryosphere
Published: 1 February 2017

estimation.

6. Conclusion

A distributed hydrological model coupled with cryospherical processes was developed in the upper Heihe basin. The model was validated using available observations of soil moisture, soil temperature, frozen depth, and streamflow discharge and was compared with remote sensing based estimation of actual evapotranspiration. Based on the model simulation from 1961 to 2013, the changes in frozen soils and the effect of the frozen soils change on hydrological processes were examined. The conclusions derived in this study are:

(1) The distributed hydrological model developed in this study accurately simulated the cryosphere hydrological processes in the upper Heihe basin, and can be used to analyze change in frozen soils and the impacts on hydrological processes on the high and cold plateau.

(2) Significant degradation of frozen soils was found in the upper Heihe basin due to the increasing air temperature over the last 50 years. The permafrost area decreased by 9.5% in the period of 1961-2013 and changed into seasonally frozen ground, especially in areas at elevation between 3500 m and 3900 m. The annual maximum frozen depth showed a significant decreasing trend of 4.1 cm/10yr in the seasonally frozen ground, and the active layer thickness increased 2.2 cm/10yr in the permafrost regions.

(3) In the freezing season (November-March), runoff was mainly subsurface flow which increased significantly in the higher elevation region due to the change in frozen soils during the study period. In the thawing season (April-October), runoff mainly

came from rainfall and showed an increasing trend at the higher elevations due to the increased precipitation. In both the freezing and thawing seasons, runoff decreased in the lower elevation region due to increased evaporation caused by rising air temperature. Since the runoff at the basin scale is mainly from the higher elevation regions, annual runoff showed a significant increasing trend due to the increased precipitation, and the base flow increased due to the degradation of frozen soils in the study period.

(4) Annual liquid water storage showed a significant increasing trend especially in the most recent three decades, due to the change in frozen soils. Annual ice water storage in the top 0-3 m of soil showed a significant decreasing trend due to soil warming. Annual groundwater storage had an increasing trend, which indicated that groundwater recharge was enhanced in the last 50 years.

(5) Regions where the permafrost changed into the seasonally frozen ground showed larger changes in runoff and soil moisture than area covered by seasonally frozen ground at low elevations.

There were uncertainties in the frozen soils and the hydrological processes simulations that might be related to the soil properties, the high spatial heterogeneity, the parameterization of the lower boundary of deep soils, which was important for simulating the permafrost thawing process, and the other factors. In addition, the interactions between the change in frozen soils, vegetation dynamics and hydrological processes need to be investigated in the future study to better understand the change in ecohydrological processes.

The Cryosphere Discuss., doi:10.5194/tc-2016-289, 2017
Manuscript under review for journal The Cryosphere
Published: 1 February 2017

Acknowledgements: This research was supported by the major plan of "Integrated Research on the Ecohydrological Processes of the Heihe Basin" (Project Nos. 91225302 and 91425303) funded by the National Natural Science Foundation of China (NSFC). The authors would like to thank the editor for their constructive comments, which greatly improved the manuscript.

References

Bartelt P. and M. Lehning: A physical snowpack model for the swiss avalanche warning: Part Ⅰ: numerical model, Cold Regions Sci. and Tech., 35(3), 123-145, doi: 10.1016/S0165-232X(02)00074-5, 2002.

Chasmer L., C. Hopkinson and W. Quinton: Quantifying errors in discontinuous permafrost plateau change from optical data, Northwest Territories, Canada: 1947–2008, Canadian Journal of Remote Sensing, 36:sup2, S211-S223, doi: 10.5589/m10-058, 2010.

Cao Y., Nan Z. and Hu X.: Estimating groundwater storage changes in the Heihe river basin using GRACE, in: IEEE International Geoscience and Remote Sensing Symposium (IGARSS), Munich, Germany, 22–27 July 2012, 798-801, 2012.

Chen, R., Lu, S., Kang, E., Ji, X., Zhang, Z., Yang, Y., Qing, W.: A distributed water-heat coupled model for mountainous watershed of an inland river basin of Northwest China (I) model structure and equations, Environ. Geol., 53, 1299-1309, doi: 10.1007/s00254-007-0738-2,2008.

Cheng, G. and Jin, H.: Permafrost and groundwater on the Qinghai-Tibet Plateau and in northeast China, Hydrogeol. J., 21, 5-23, doi: 10.1007/s10040-012-0927-2, 2013.

Cheng, G., Li, X., Zhao, W., Xu, Z., Feng, Q., Xiao, S., Xiao, H.: Integrated study of the water-

The Cryosphere Discuss., doi:10.5194/tc-2016-289, 2017
Manuscript under review for journal The Cryosphere
Published: 1 February 2017

ecosystem-economy in the Heihe River Basin. Nat. Sci. Rev., 1(3), 413-428, doi: 10.1093/nsr/nwu017, 2014.

Cheng, G., and Wu T.: Responses of permafrost to climate change and their environmental significance, Qinghai-Tibet Plateau, J. Geophys. Res., 112, F02S03, doi:10.1029/2006JF000631, 2007.

Cherkauer, K. A., and D. P. Lettenmaier: Hydrologic effects of frozen soils in the upper Mississippi River basin, J. Geophys. Res., 104, 19,599-19,610, doi: 10.1029/1999JD900337, 1999.

Cuo, L., Y. Zhang, F. Zhu, and L. Liang.: Characteristics and changes of streamflow on the Tibetan Plateau: A review, J. Hydrol.: Reg. Stud., 2, 49-68, doi: 10.1016/j.ejrh.2014.08.004, 2014.

Cuo, L., Y. Zhang, T. J. Bohn, L. Zhao, J. Li, Q. Liu, and B. Zhou: Frozen soil degradation and its effects on surface hydrology in the northern Tibetan Plateau, J. Geophys. Res. Atmos., 120, doi:10.1002/2015JD023193, 2015.

Fan, W.: Heihe 1km LAI production, Heihe Plan Science Data Center at Lanzhou, doi:10.3972/heihe.090.2014.db, 2014.

Farouki, O.T.: The thermal properties of soils in cold regions, Cold Regions Sci.and Tech., 5, 67-75, doi: 10.1016/0165-232X(81)90041-0, 1981.

Flerchinger G., Saxton K.: Simultaneous heat and water model of a freezing snow-residue-soil system I. Theory and development, Trans. ASAE, 32, 565-571, doi: 10.13031/2013.31040, 1989.

Gao B., Qin Y., Wang YH, Yang DW, and Zheng YR: Modeling Ecohydrological Processes and Spatial Patterns in the Upper Heihe Basin in China, Forests, 7(1),10, doi:10.3390/f7010010, 2016.

Jacques St., J.-M., and Sauchyn D. J.: Increasing winter baseflow and mean annual streamflow from possible permafrost thawing in the Northwest Territories, Canada, Geophys. Res. Lett., 36, L01401, doi:10.1029/2008GL035822, 2009.

Jarvis, A., Reuter, H.I., Nelson, A., Guevara, E.: Hole-filled seamless SRTM data, Version 4, International Centre for Tropical Agriculture (CIAT), 2008.

Jin, H., He, R., Cheng, G., Wu, Q., Wang, S., Lu, L. and Chang X.: Changes in frozen ground in the Source Area of the Yellow River on the Qinghai–Tibet Plateau, China, and their eco-environmental impacts, Environ. Res. Lett., 4(4), 045206, doi:10.1088/1748-9326/4/4/045206, 2009.

Jin, H.J., Zhao, L., Wang, S.L., Jin, R.: Thermal regimes and degradation modes of permafrost along the Qinghai–Tibet Highway, Science in China D: Earth Sciences, 49 (11), 1170-1183, 2006.

Jordan R.: A one-dimensional temperature model for a snow cover, Technical Documentation for SNTHERM.89, Cold Regions Research and Engineering Lab, Hanover NH, 49 pp., 1991.

Jorgenson, M. T., Y. L. Shur, and E. R. Pullman: Abrupt increase in permafrost degradation in Arctic Alaska, Geophys. Res. Lett., 33, L02503, doi:10.1029/2005GL024960, 2006.

Lawrence, D.M., C.D. Koven, S.C. Swenson, W.J. Riley, and A.G. Slater: Permafrost thaw and resulting soil moisture changes regulate projected high-latitude CO_2 and CH_4 emissions, Environ. Res. Lett., 10, doi:10.1088/1748-9326/10/9/094011, 2015.

Li, D.L., Zhong, H.L., Wu, Q.B., Zhang, Y.J., Hou, Y.L., Tang, M.C.: Analyses on changes of surface temperature over Qinghai–Xizang Plateau, Plateau Meteorology, 24, 291-298, 2005 (in Chinese).

Li, X., Cheng, G.D., Liu, S.M., Xiao, Q., Ma, M.G., Jin, R., Che, T., Liu, Q.H., Wang, W.Z., Qi, Y., Wen, J.G., Li, H.Y., Zhu, G.F., Guo, J.W., Ran, Y.H., Wang, S.G., Zhu, Z.L., Zhou, J., Hu, X.L., Xu, Z.W.: Heihe Watershed Allied Telemetry Experimental Research (HiWATER): Scientific Objectives and Experimental Design, B. Am. Meteorol. Soc., 94(8), 1145-1160, doi: 10.1175/BAMS-D-12-00154.1, 2013.

Liu, X. and Chen, B.: Climate warming in the Tibetan Plateau during recent decades, Int. J. Climatol., 20(1), 1729-1742, doi: 10.1002/1097-0088(20001130)20:14<1729::AID-JOC556>3.0.CO;2-, 2000.

Liu, S., Xu Z., Wang W., Bai J., Jia Z., Zhu M., and Wang J.: A comparison of eddy-covariance and large aperture scintillometer measurements with respect to the energy balance closure problem, Hydrol. Earth Syst. Sc., 15(4), 1291-1306, doi:10.5194/hess-15-1291-2011, 2011.

Liu J., N. Hayakawab, Lu M., Dong S., and Yuan J.: Hydrological and geocryological response of winter streamflow to climate warming in Northeast China, Cold Regions Sci.and Tech., 37,15-24, doi: 10.1016/S0165-232X(03)00012-0, 2003.

Wu T., Li S., Cheng G. and N Z.: Using ground-penetrating radar to detect permafrost degradation in the northern limit of permafrost on the Tibetan Plateau, Cold Regions Sci.and Tech., 41, 211-219, 2005, doi:10.1016/j.coldregions.2004.10.006.

Niu L., Ye B., Li J., and Sheng Y.: Effect of permafrost degradation on hydrological processes in typical basins with various permafrost coverage in Western China, China Earth Sci., 54(4), 615-624, doi: 10.1007/s11430-010-4073-1, 2011.

Oerlemans, J. and Knap, W.H.: A 1 year record of global radiation and albedo in the ablation zone of Morteratschgletscher, Switzerland, J. Glaciol., 44, 231-238, doi: 10.3198/1998JoG44-147-231-238, 1998.

Oerlemans, J.: Glaciers and Climate Change, Lisse: Swets & Zeitlinger, 2001.

Oleson, K.W., Lawrence, D.M., Bonan, G.B., Flanner, M.G., Kluzek, E., Lawrence, P.J., Levis, S., Swenson, S.C., Thornton, P.E., Dai, A., Decker, M., Dickinson, R., Feddema, J., Heald, C.L., Hoffman, F., Lamarque, J., Mahowald, N., Niu, G., Qian, T., Randerson, J., Running, S., Sakaguchi, K., Slater, A., Stöckli, R., Wang, A., Yang, Z., Zeng, X., Zeng, X.: Technical Description of version 4.0 of the Community Land Model (CLM), NCAR Technical Note NCAR/TN-47+STR, National Center for Atmospheric Research, Boulder, CO, 257 pp., 2010.

Qiu J.: Thawing permafrost reduces river runoff, Nature, doi:10.1038/nature.2012.9749, 2012.

Rawlins M., Lammers R., Frolking S., Fekete B. and Vorosmarty C.: Simulating pan-Arctic runoff with a macro-scale terrestrial water balance model, Hydrol. Process., 17, 2521-2539, doi: 10.1002/hyp.1271, 2003.

Rawlins, M.A., D.J. Nicolsky, K.C. McDonald, and V.E. Romanovsky: Simulating soil freeze/thaw dynamics with an improved pan-Arctic water balance model, J. Adv. Model. Earth Syst., 5:659-675, doi:10.1002/jame.20045, 2013.

Rigon R., Bertoldi G., and Over TM: GEOtop: A distributed hydrological model with coupled water and energy budgets, J. Hydrometeorol., 7, 371–388, doi: 10.1175/JHM497.1, 2006.

Sellers, P.J.: Canopy reflectance, photosynthesis, and transpiration, Int. J. Remote Sens., 8, 1335-1372, doi: 10.1080/01431168508948283, 1985.

Sellers, P.J.; Randall, D.A.; Collatz, G.J.; Berry, J.A.; Field, C.B.; Dazlich, D.A.; Zhang, C.; Collelo, G.D.; Bounoua, L.: A Revised Land Surface Parameterization (SiB2) for Atmospheric GCMS. Part I: Model Formulation, J. Clim., 9, 676-705, doi: 10.1175/1520-0442(1996)009<0676:ARLSPF>2.0.CO;2, 1996.

Shen, Y. and Xiong, A.: Validation and comparison of a new gauge-based precipitation analysis over mainland China, Int. J. Climatol., 36, 252-265, doi: 10.1002/joc.4341, 2015.

Song X., Brus DJ, Liu F., Li D., Zhao Y., Yang J. and Zhang G.: Mapping soil organic carbon content by geographically weighted regression: A case study in the Heihe River Basin, China, Geoderma, 261,11–22, doi: 10.1016/j.geoderma.2015.06.024, 2016.

Subin Z.M., Koven C.D., Riley W.J., Torn M.S., Lawrence D.M. and Swenson S.C.: Effects of Soil Moisture on the Responses of Soil Temperatures to Climate Change in Cold Regions, J. Clim., 26,3139-3158, doi: 10.1175/JCLI-D-12-00305.1, 2013.

Toon, O.B., McKay, C.P., Ackerman, T.P., and Santhanam, K.: Rapid calculation of radiative heating rates and photodissociation rates in inhomogeneous multiple scattering atmospheres, J. Geophys. Res. 94(D13), 16,287-16,301, doi: 10.1029/JD094iD13p16287, 1989.

Walter W. Immerzeel, Ludovicus P. H. van Beek, and Marc F. P. Bierkens.: Climate Change Will Affect the Asian Water Towers, Science, 328, 1382-1385, doi: 10.1126/science.1183188, 2010.

Walvoord, M. A. and B. L. Kurylyk: Hydrologic Impacts of Thawing Permafrost—A Review, Vadose Zone J., doi:10.2136/vzj2016.01.0010, 2016.

Wang, L., Koike, T., Yang, K., Jin, R., Li, H.: Frozen soil parameterization in a distributed biosphere hydrological model, Hydrol. Earth Syst. Sc., 14(3), 557-571, doi: 10.5194/hess-14-557-2010, 2010.

Wang Q., Zhang T., Wu J., et al.: Investigation of permafrost distribution over the upper reaches of the Heihe River in the Qilian Mountains, Journal of Glaciology and Geocryology, 35(1), 19-29, 2013 (in Chineses).

Wang Q., Zhang T., Peng X., Cao B., and Wu Q.: Changes of soil thermal regimes in the Heihe River Basin over Western China, Arct., Antarct., and Alpine Res., 47(2), 231-241, doi: 10.1657/AAAR00C-14-012, 2015a.

Wang, Y.; Yang, D.; Lei, H. and Yang, H.: Impact of cryosphere hydrological processes on the river runoff in the upper reaches of Heihe River, J. Hydraul. Eng., 46, 1064-1071, 2015b (In Chinese).

Woo, M.-K., Kane, D. L., Carey, S. K. and Yang, D.: Progress in permafrost hydrology in the new millennium, Permafrost Periglac. Process., 19, 237-254, doi:10.1002/ppp.613, 2008.

Woo M K.: Permafrost Hydrology, Springer-Verlag, Berlin Heidelberg, 2012.

Wu, B.F., Yan, N.N., Xiong, J., Bastiaanssen, W., Zhu, W.W., Stein, A.: Validation of ETWatch using field measurements at diverse landscapes: A case study in Hai Basin of China. J. Hydrol., 436, 67-80, doi: 10.1016/j.jhydrol.2012.02.043, 2012.

Wu, B.F.: Monthly Evapotranspiration Datasets (2000–2012) with 1 km Spatial Resolution over the Heihe River Basin, Heihe Plan Science Data Center at Lanzhou, China, doi: 10.3972/heihe.115.2013.db, 2013.

Wu, Q., and Zhang T.: Changes in active layer thickness over the Qinghai-Tibetan Plateau from 1995 to 2007, J. Geophys. Res., 115, D09107, doi: 10.1029/2009JD012974, 2010.

Yang, D.W., Gao, B., Jiao, Y., Lei, H.M., Zhang, Y.L., Yang, H.B., Cong, Z.T.: A distributed scheme developed for eco-hydrological modeling in the upper Heihe River, China Earth Sci., 58(1), 36-45, doi: 10.1007/s11430-014-5029-7, 2015.

Yang, D.W., Herath, S., and Musiake, K.: Development of a geomorphology-based hydrological model for large catchments, Annu. J. Hydraul. Eng., 42, 169-174, doi: 10.2208/prohe.42.169, 1998.

Yang, D.W., Herath, S., and Musiake, K.: A hillslope-based hydrological model using catchment area and width functions, Hydrol. Sci. J., 47, 49-65, doi: 10.1080/02626660209492907, 2002.

Yang, M., F. E. Nelson, N. I. Shiklomanov, D. Guo, and G. Wan, Permafrost degradation and its environmental effects on the Tibetan Plateau: A review of recent research, Earth Sci. Rev., 103, 31-44, doi: 10.1016/j.earscirev.2010.07.002, 2010.

Ye, B., D. Yang, Z. Zhang, and D. L. Kane: Variation of hydrological regime with permafrost coverage over Lena Basin in Siberia, J. Geophys. Res., 114, D07102, doi:10.1029/2008JD010537, 2009.

Zhao, L., C. L. Ping, D. Q. Yang, G. D. Cheng, Y. J. Ding, and S. Y. Liu: Changes of climate and seasonally frozen ground over the past 30 years in Qinghai-Xizang (Tibetan) Plateau, China, Global Planet. Change, 43, 19-31, doi: 10.1016/j.gloplacha.2004.02.003, 2004.

Zhang, Y.L., Cheng, G.D., Li, X., Han, X.J., Wang, L., Li, H.Y., Chang, X.L., Flerchinger, G.N.: Coupling of a simultaneous heat and water model with a distributed hydrological model and

The Cryosphere Discuss., doi:10.5194/tc-2016-289, 2017
Manuscript under review for journal The Cryosphere
Published: 1 February 2017

evaluation of the combined model in a cold region watershed, Hydrol. Process., 27(25), 3762-3776, doi: 10.1002/hyp.9514, 2013.

Zhang, Y., Ohata, T., and Kadota, T.: Land-surface hydrological processes in the permafrost region of the eastern Tibetan Plateau, J. Hydrol., 283, 41-56, doi: 10.1016/S0022-1694(03)00240-3, 2003.

Zhou, J.H. and Zheng, Y.R.: Vegetation Map of the upper Heihe basin, Version 2.0, Heihe Plan Science Data Center at Lanzhou, China, doi:10.3972/heihe.426.2014.db, 2014.

Figure caption:

Figure 1. The Study area, hydrological stations, borehole observation and flux tower stations

Figure 2. Comparison of the simulated and the observed soil temperature at borehole observation sites, and the observed data is provided by Wang et al. (2013)

Figure 3. Daily soil temperature at the Qilian station: (a) observation; (b) simulation; (c) Simulation-Observation

Figure 4. Comparison of the simulated and observed daily frozen depths during the period of 2002-2014 at: (a) the Qilian station, (b) the Yeniugou station

Figure 5. Comparison of the simulated and the observed hourly liquid soil moisture at the A'rou Sunny Slope station

Figure 6. Comparison of the simulated and the observed daily river discharge at: (a) the Yingluoxia Gauge, (b) the Qilian Gauge, and (c) the Zhamashike Gauge.

Figure 7. Comparison of the simulated and the remote sensing estimated actual evapotranspiration in the period of 2002~2012

Figure 8. Changes of the mean soil temperature in different seasons: (a) the freezing season (from November to March) (b) the thawing season (from April to October)

Figure 9. Change of the frozen soils in the upper Heihe basin: (a) areas of permafrost and basin averaged annual air temperature; (b) the basin averaged annual maximum frozen depth of the seasonally frozen ground and the annual maximum thaw depth of the permafrost

Figure 10. Figure 10. Distribution of permafrost and seasonally frozen ground: (a) distribution in the period of 1971-1980; (b) distribution in the period of 2001-2010; (c) percentage of areas of permafrost and seasonally frozen ground at sunny slope; (d) percentage of areas of permafrost and

The Cryosphere Discuss., doi:10.5194/tc-2016-289, 2017
Manuscript under review for journal The Cryosphere
Published: 1 February 2017

seasonally frozen ground at shaded slope (the same legend as (c))

Figure 11. Spatial averaged monthly soil temperature during the period of 1961-2013 in different elevation intervals: (a) the seasonally frozen ground with elevation between 3300-3500 m; (b) the areas where permafrost changed to seasonally frozen ground with elevation between 3500-3700 m

Figure 12. Changes of the runoff and actual evapotranspiration: (a) in the freezing season; (b) in the thawing season

Figure 13. Changes of the annual water storage (equivalent water depth) during the period of 1961-2013: (a) the liquid soil water storage of the top 0-3 m layer; (b) the ice water storage of the top 0-3 m layer; (c) the groundwater storage

Figure 14. Spatial averaged monthly liquid soil moisture during the period of 1961-2013 in different elevation intervals: (a) the seasonally frozen ground with elevation between 3300-3500 m; (b) the areas where permafrost changed to seasonally frozen ground with elevation between 3500-3700 m

Figure 15. Model simulated changes of runoff: (a) in the freezing season, (b) in the thawing season

The Cryosphere Discuss., doi:10.5194/tc-2016-289, 2017
Manuscript under review for journal The Cryosphere
Published: 1 February 2017

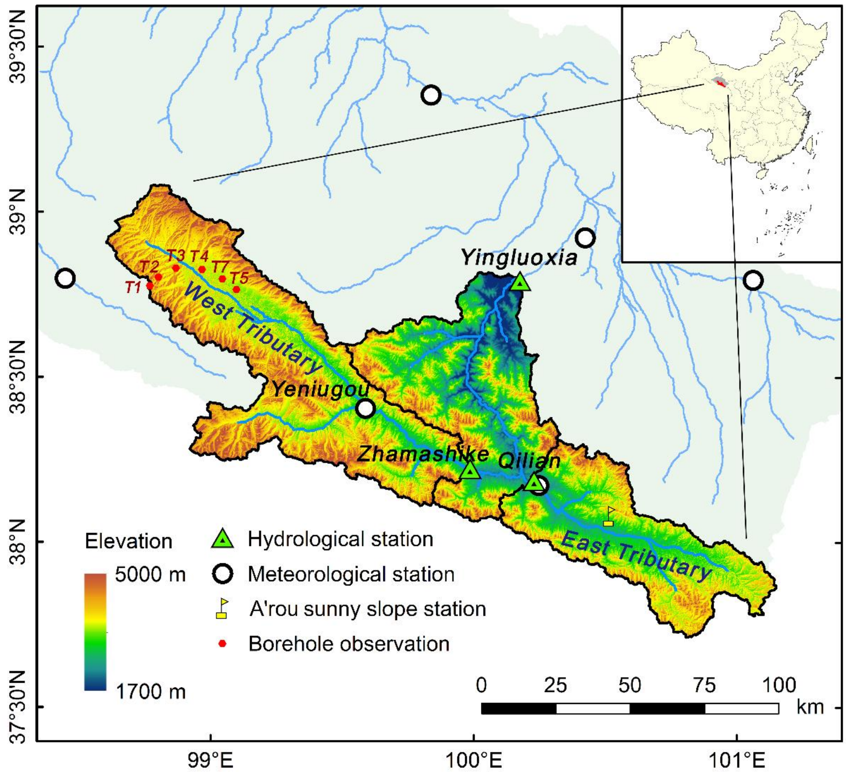

Figure 1. The Study area, hydrological stations, borehole observation and flux tower stations

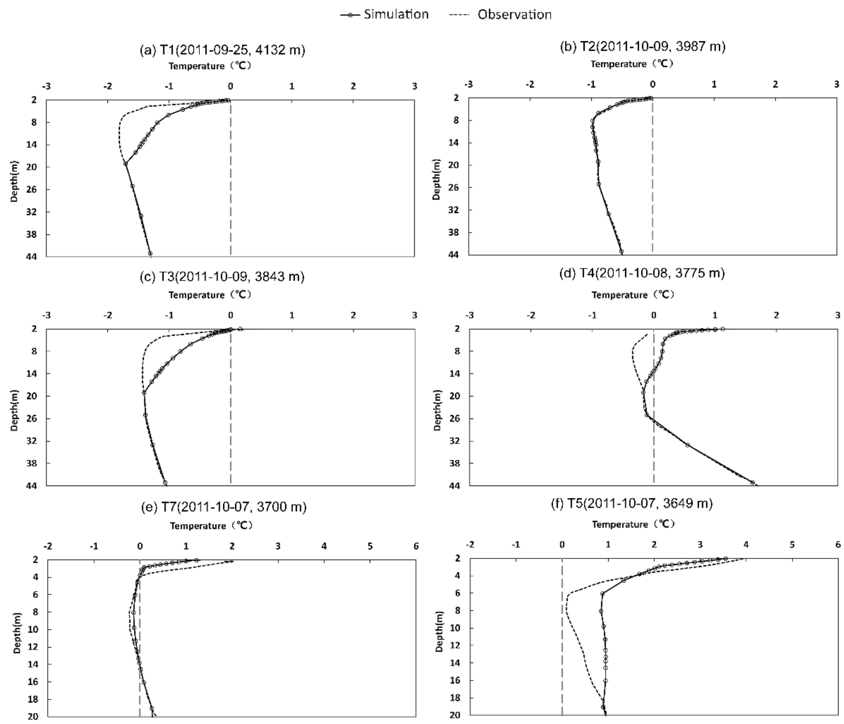

Figure 2. Comparison of the simulated and the observed soil temperature at borehole observation sites, and the observed data is provided by Wang et al. (2013)

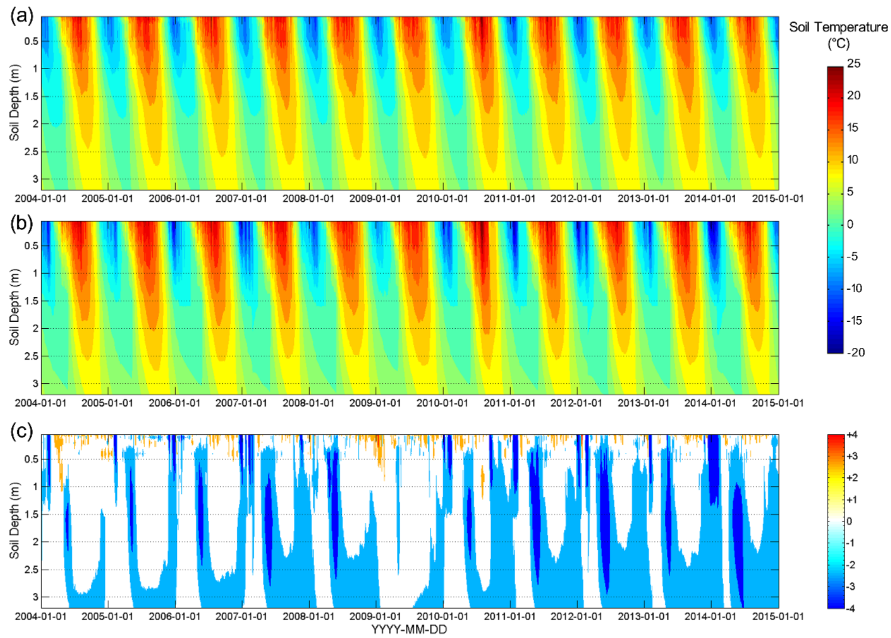

Figure 3 Daily soil temperature at the Qilian station: (a) observation; (b) simulation; (c) Simulation-Observation

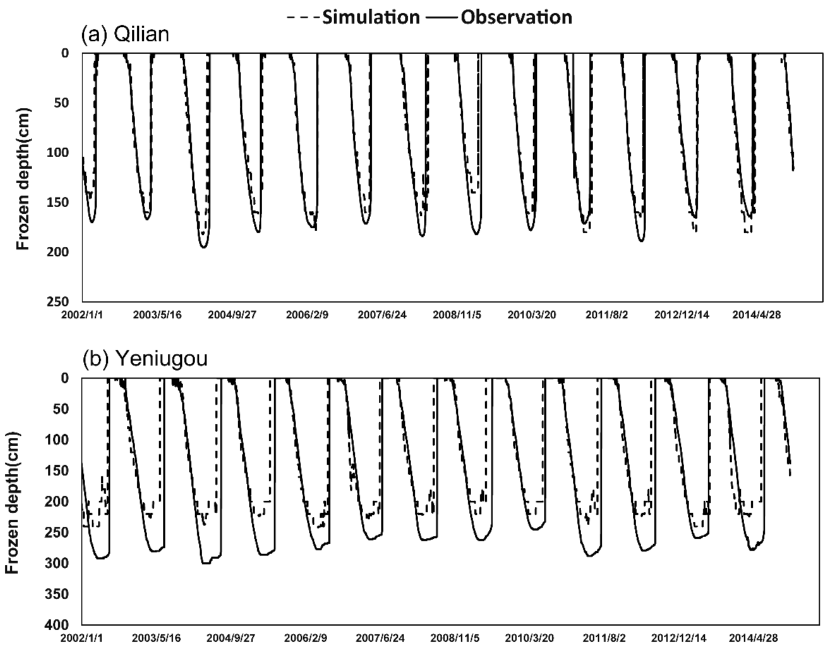

Figure 4. Comparison of the simulated and observed daily frozen depths during the period of 2002-2014 at: (a) the Qilian station, (b) the Yeniugou station

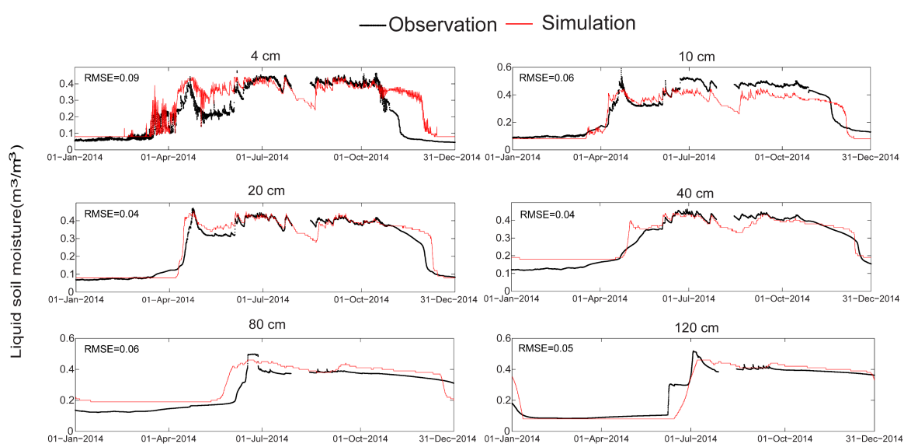

Figure 5. Comparison of the simulated and the observed hourly liquid soil moisture at the A'rou Sunny Slope station

The Cryosphere Discuss., doi:10.5194/tc-2016-289, 2017
Manuscript under review for journal The Cryosphere
Published: 1 February 2017

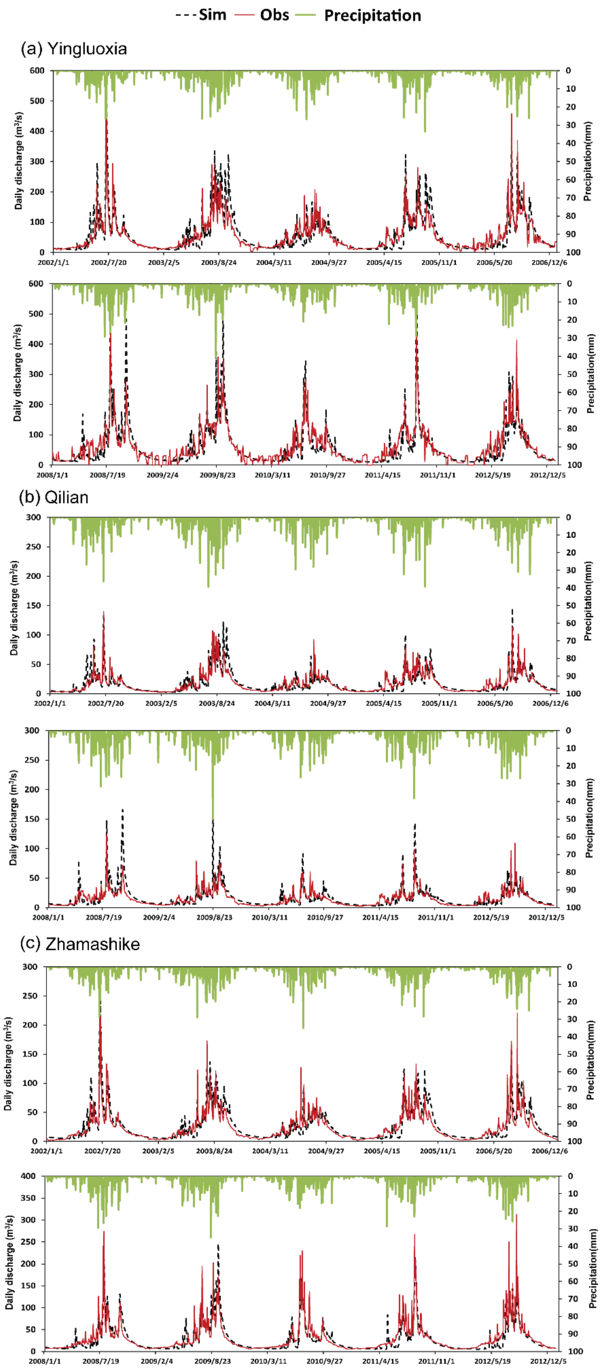

831

832 Figure 6. Comparison of the simulated and the observed daily river discharge at: (a)

833 the Yingluoxia Gauge, (b) the Qilian Gauge, and (c) the Zhamashike Gauge.

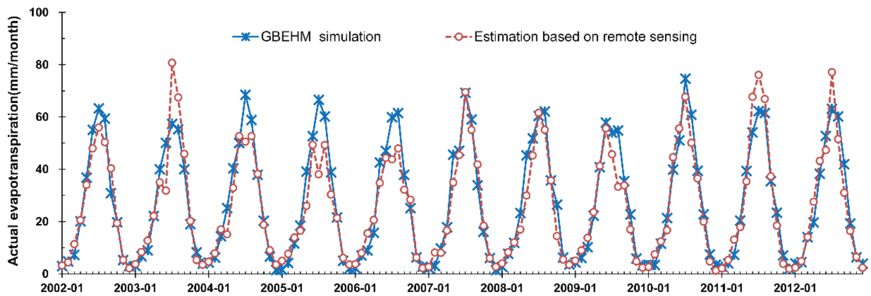

Figure 7. Comparison of the simulated and the remote sensing estimated actual evapotranspiration in the period of 2002~2012

The Cryosphere Discuss., doi:10.5194/tc-2016-289, 2017
Manuscript under review for journal The Cryosphere
Published: 1 February 2017

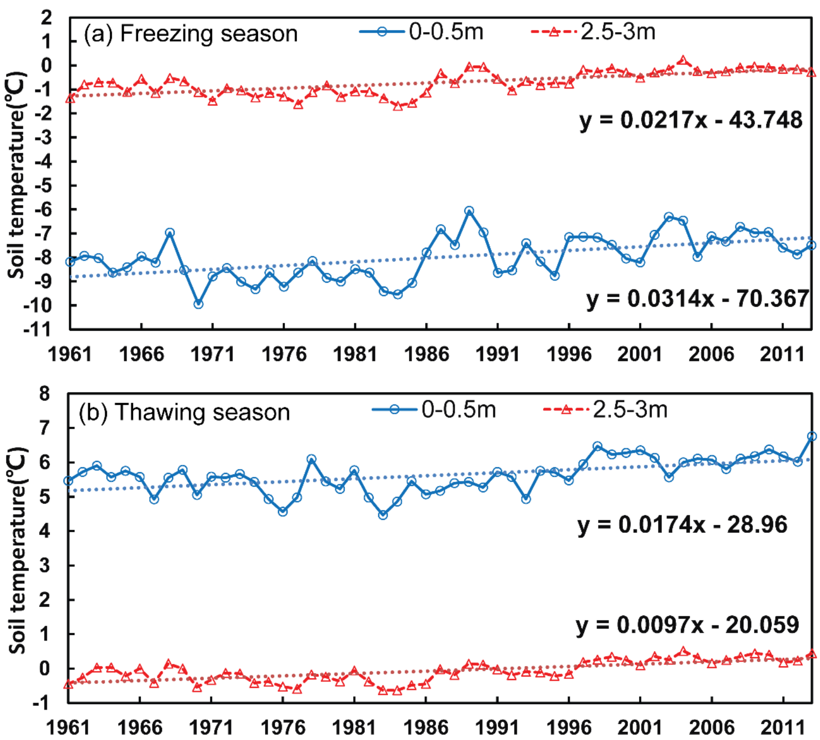

Figure 8. Changes of the mean soil temperature in different seasons: (a) the freezing season (from November to March) (b) the thawing season (from April to October)

The Cryosphere Discuss., doi:10.5194/tc-2016-289, 2017
Manuscript under review for journal The Cryosphere
Published: 1 February 2017

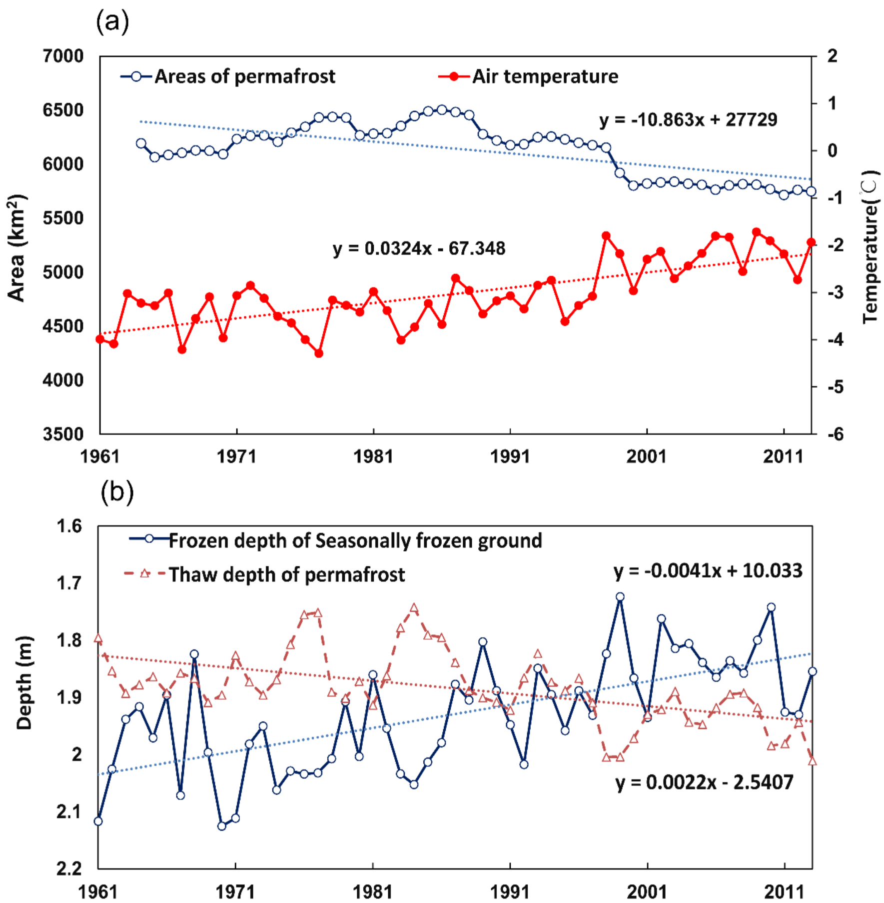

Figure 9. Change of the frozen soils in the upper Heihe basin: (a) areas of permafrost and basin averaged annual air temperature; (b) the basin averaged annual maximum frozen depth of the seasonally frozen ground and the annual maximum thaw depth of the permafrost

The Cryosphere Discuss., doi:10.5194/tc-2016-289, 2017
Manuscript under review for journal The Cryosphere
Published: 1 February 2017

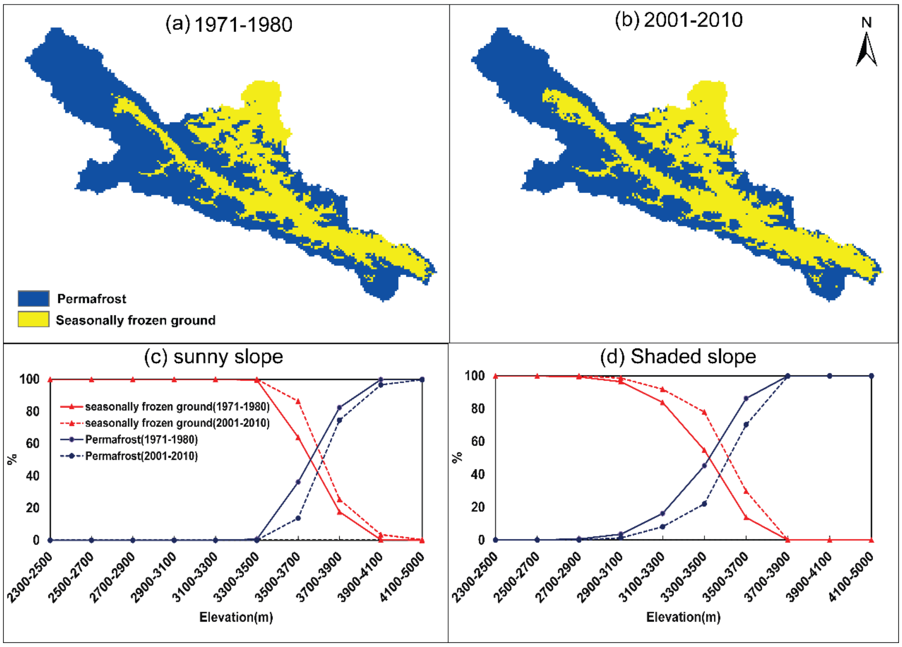

Figure 10. Distribution of permafrost and seasonally frozen ground: (a) distribution in the period of 1971-1980; (b) distribution in the period of 2001-2010; (c) percentage of areas of permafrost and seasonally frozen ground at sunny slope; (d) percentage of areas of permafrost and seasonally frozen ground at shaded slope (the same legend as (c))

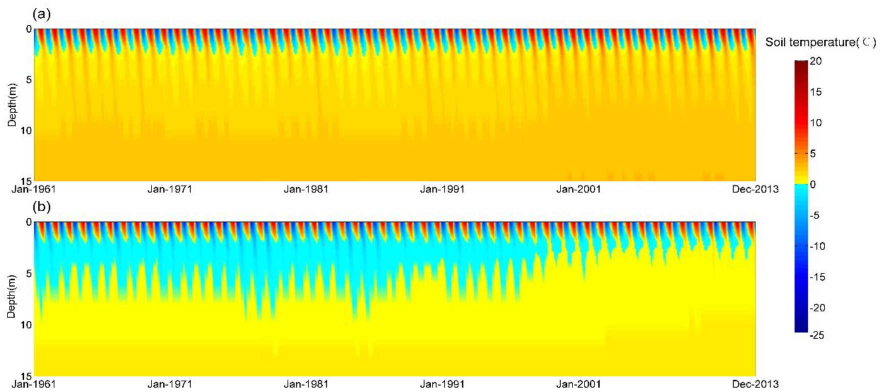

Figure 11. Spatial averaged monthly soil temperature during the period of 1961-2013 in different elevation intervals: (a) the seasonally frozen ground with elevation between 3300-3500 m; (b) the areas where permafrost changed to seasonally frozen ground with elevation between 3500-3700 m

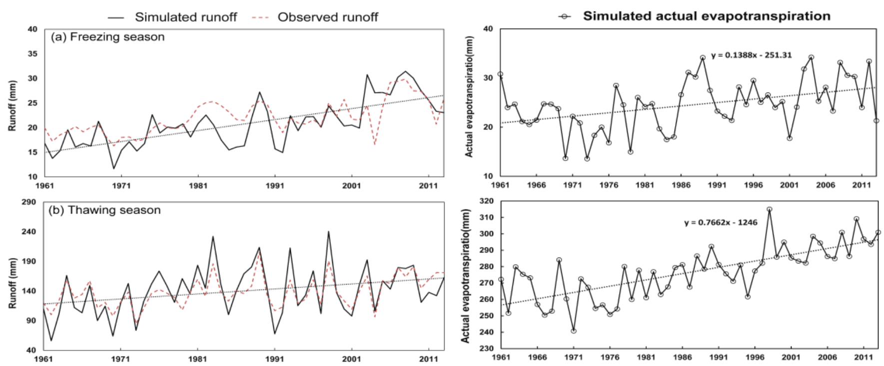

Figure 12. Changes of the runoff and actual evapotranspiration: (a) in the freezing season; (b) in the thawing season

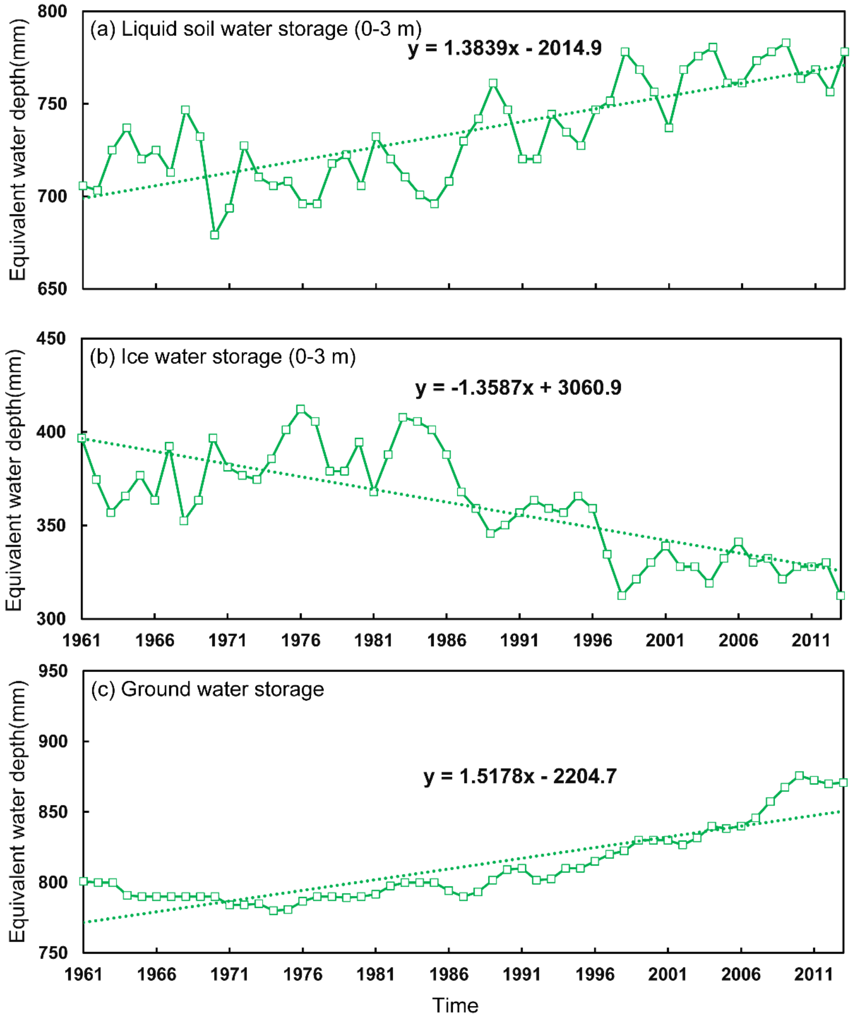

872

873 Figure 13. Changes of the annual water storage (equivalent water depth) during the
874 period of 1961-2013: (a) the liquid soil water storage of the top 0-3 m layer; (b) the ice
875 water storage of the top 0-3 m layer; (c) the groundwater storage

The Cryosphere Discuss., doi:10.5194/tc-2016-289, 2017
Manuscript under review for journal The Cryosphere
Published: 1 February 2017

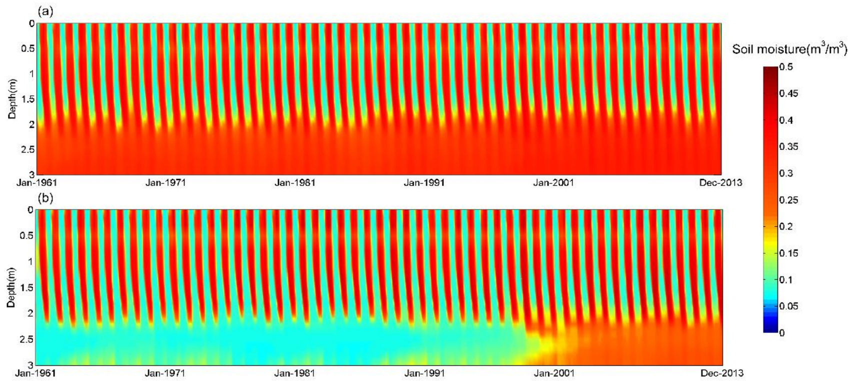

Figure 14. Spatial averaged monthly liquid soil moisture during the period of 1961-2013 in different elevation intervals: (a) the seasonally frozen ground with elevation between 3300-3500 m; (b) the areas where permafrost changed to seasonally frozen ground with elevation between 3500-3700 m

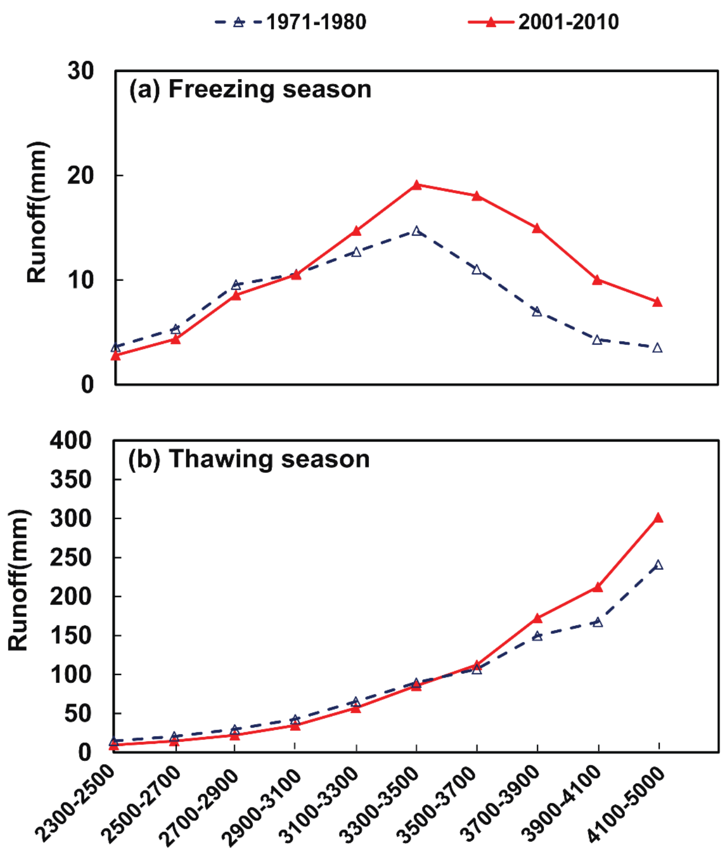

Figure 15. Model simulated changes of runoff: (a) in the freezing season, (b) in the thawing season

The Cryosphere Discuss., doi:10.5194/tc-2016-289, 2017
Manuscript under review for journal The Cryosphere
Published: 1 February 2017

Table list:

899 Table 1 Major parameters of the GBEHM model

Parameters	Coniferous Forest	Shrub	Steppe	Alpine Meadow	Alpine Sparse Vegetation	Desert
Surface retention capacity (mm)	30.0	25.0	10.0	15.0	15.0	5.0
Surface roughness (Manning coefficient)	0.5	0.3	0.1	0.1	0.1	1.0
Soil reflectance to visible light	0.20	0.20	0.20	0.28	0.14	0.11
Soil reflectance to near-infrared radiation	0.225	0.225	0.225	0.28	0.225	0.225
Leaf reflectance to visible light	0.105	0.105	0.105	0.105	0.105	—
Leaf reflectance to near-infrared radiation	0.35	0.58	0.58	0.58	0.58	—
Leaf transmittance to visible light	0.05	0.07	0.07	0.07	0.07	—
Leaf transmittance to near-infrared radiation	0.10	0.25	0.25	0.25	0.25	—
Maximum Rubsico capacity of top leaf (10^{-5} mol m^{-2} s^{-1})	6.0	6.0	3.3	3.3	3.0	—
Plant root depth (m)	2.0	1.0	0.40	0.40	0.1	0.0
Intrinsic quantum efficiency (mol mol^{-1})	0.08	0.08	0.05	0.05	0.05	—
Canopy top height (m)	9.0	1.9	0.3	0.3	0.2	—
Leaf length (m)	0.055	0.055	0.3	0.3	0.04	—
Leaf width (m)	0.001	0.001	0.005	0.005	0.001	—
Stem area index	0.08	0.08	0.05	0.05	0.08	—

900
901
902
903 Table 2 Model performance of the daily streamflow simulation

Station	Calibration period (2002~2006)		Validation period (2008~2012)	
	NSE	RE (%)	NSE	RE (%)
Yingluoxia	0.64	3.8	0.65	-5.6
Qilian	0.65	1.5	0.60	9.3
Zhamashike	0.70	9.9	0.75	-7.0

904
905

The Cryosphere Discuss., doi:10.5194/tc-2016-289, 2017
Manuscript under review for journal The Cryosphere
Published: 1 February 2017

Table 3 Changes in basin water balance

Decade	Precipitation (mm/yr)	Actual evaporation (mm/yr)	Simulated runoff (mm/yr)	Observed runoff (mm/yr)	Runoff ratio(observed)	Runoff ratio (simulated)
1961-1970	405.7	288.8	133.3	144.1	0.36	0.33
1971-1980	439.1	280.8	154.5	143.8	0.33	0.35
1981-1990	492.8	300.0	186.2	174.1	0.35	0.38
1991-2000	471.0	306.1	160.1	157.4	0.33	0.34
2001-2010	504.3	317.4	177.9	174.3	0.35	0.35

Table 4 Changes in runoff components in different seasons

Freezing season (from November to March)			
	Total runoff (mm)	Glacier runoff (mm)	Snowmelt runoff (mm)
1961-1970	16.5	0.0	0.0
1971-1980	18.5	0.0	0.0
1981-1990	20.2	0.0	0.0
1991-2000	20.4	0.0	0.0
2001-2010	27.2	0.0	0.0
Thawing season (from April to October)			
	Total runoff (mm)	Glacier runoff (mm)	Snowmelt runoff (mm)
1961-1970	116.8	3.0	26.2
1971-1980	136.0	3.5	13.5
1981-1990	166.1	3.1	28.2
1991-2000	139.7	3.8	19.2
2001-2010	150.7	3.7	25.8

Table 5 Correlation between runoff/soil moisture and precipitation/soil temperature

	Freezing season			Thawing season		
	P	Tsoil	LSM	P	Tsoil	LSM
LSM	0.26	0.89	-	0.61	0.85	-
Runoff	0.30	0.66	0.82	0.93	0.06	0.43

Note: P is the precipitation, Tsoil is the mean soil temperature of 0-3 m, LSM is the mean liquid soil moisture of 0-3 m.